

Suppression of $1/f$ noise in graphene due to non-scalar mobility fluctuations induced by impurity motion

Masahiro Kamada,¹ Weijun Zeng,^{1,2} Antti Laitinen,¹ Jayanta Sarkar,¹
Sheng-Shiuan Yeh,³ Kirsi Tappura,^{4,5} Heikki Seppä,⁴ and Pertti Hakonen^{1,2}

¹*Low Temperature Laboratory, Department of Applied Physics,
Aalto University School of Science,
P.O. Box 15100, 00076 Aalto, Finland*

²*QTF Centre of Excellence, Department of Applied Physics,
Aalto University 00076 Aalto, Finland*

³*International College of Semiconductor Technology,
National Yang Ming Chiao Tung University, Hsinchu City, Taiwan*

⁴*Microelectronics and quantum technology,
VTT Technical Research Centre of Finland Ltd.,
P.O. Box 1000, 02044 VTT, Finland*

⁵*Microelectronics and quantum technology,
VTT Technical Research Centre of Finland Ltd.,
QTF Centre of Excellence, P.O. Box 1000, 02044 VTT, Finland*

(Dated: December 23, 2021)

Abstract

Low frequency resistance variations due to mobility fluctuations is one of the key factors of $1/f$ noise in metallic conductors. According to theory, such noise in a two-dimensional (2D) device can be suppressed to zero at small magnetic fields, implying important technological benefits for low noise 2D devices. In this work, we provide direct evidence of anisotropic mobility fluctuations by demonstrating a strong field-induced suppression of noise in a high-mobility graphene Corbino disk, even though the device displays only a tiny amount of $1/f$ noise inherently. The suppression of the $1/f$ noise depends on charge density, showing less non-uniform mobility fluctuations away from the Dirac point with charge puddles. We model our results using a new approach based on impurity clustering dynamics and find our results consistent with the $1/f$ noise induced by scattering of carriers on mobile impurities forming clusters.

Modeling of $1/f$ noise is a challenging task that has been investigated intensively since the invention of semiconducting transistors in the late 1940's. Typically, models based on a collection of two-level systems (TLS) or trap states are employed^{1,2}. Using a large collection of such states with broadly distributed parameters, wide band $1/f$ noise can be generated. In particular, analysis of low frequency noise in terms of charge traps in transport channels in field effect transistors has been very successful².

According to the commonly accepted view, the $1/f$ noise in metallic conductors is determined entirely by fluctuations in charge carrier mobility³. Several models have been put forward to elucidate the mobility noise. Apart from the models based on localized states and fluctuating scattering cross sections⁴, models based on modification of electron interference by mobile defects have been quite successful in accounting for many experimental observations^{5,6}. Furthermore, noise due to agglomeration of impurities have been investigated using master equation⁷ and lattice gas⁸ type of approaches, and noise close to $1/f$ spectrum has been obtained.

In the present experimental work, our aim is to investigate the generic nature of $1/f$ noise in high-quality graphene. We will demonstrate that major part of the noise originates from mobility fluctuations, the effect of which depends on the magnetic field. Mobility fluctuations can be modeled by moving impurities or moving defects, which leads to universal characteristics due to impurity dynamics that we compare with our results. For example, the dynamics of mobile impurities may lead to genuine long-time correlations which may dominate the low-frequency noise under favorable conditions instead of a combination of random single fluctuators⁹. Long-time memory effects are naturally offered by the nearly endless number of possible reconfigurations among a collection of mobile impurities. The reshaping of impurity clusters via infrequent hopping events across large energy barriers leads to long-term, non-exponential correlations, which yields $1/f$ noise over large frequency spans.

Recent experiments imply that the origin of $1/f$ noise in graphene is complex, in particular near the charge neutrality point (Dirac point)^{10,11}. The noise is argued to arise from an interplay of charge traps, atomic defects, short and long range scattering, as well as charge puddles. Various models have been proposed, and qualitative agreement with the data has been reached¹²⁻¹⁸. In many graphene devices, even correlations between charge traps and mobility noise have been found^{19,20}, which is also common in regular metallic and

semiconducting devices^{1,4,21}. In our work, suspended clean graphene removes many of these noise sources and the fundamental noise elements can be addressed in pure form.

Corbino geometry is unique for electrical transport as the magnetoresistance includes only the diagonal conductivity component σ_{xx} . This feature means that, if there are isotropic mobility fluctuations (fully correlated in two orthogonal directions) causing $1/f$ noise, this noise component will be suppressed to zero at $\mu_0 B = 1$ ²²; here μ_0 denotes the mobility at $B = 0$. This behavior has unsuccessfully been searched for both in two-dimensional electron gas^{23–26} as well as in graphene²⁷. Our experimental results display a clear suppression of noise as a function of B , with a minimum around $\mu_0 B \simeq 1$. This is direct proof that a large part of the $1/f$ noise originates from mobility fluctuations in clean graphene.

I. 1/F NOISE

In metallic materials, the power spectral density of $1/f$ fluctuations is often assigned to the random impurity scattering due to the mobile impurities, defects, or vacancies²⁸. Accordingly, the spectral density of $1/f$ noise $S_m(f)$ is related to fluctuations of the conductivity σ_m governed by mobile impurities,

$$S_m(f) = \frac{\langle \Delta \sigma_m^2 \rangle}{\sigma_m^2} = \frac{\langle \Delta \mu_m^2 \rangle}{\mu_m^2} = \mathbf{s}_m \frac{1}{f}, \quad (1)$$

where $\sigma_m = e\mu_m n$ with μ_m limited by scattering of the mobile impurities alone, e is the electron charge, and $\mathbf{s}_m = \text{const.}$ (when the number of impurities is fixed), i.e. the noise does not scale with the density of charge carriers n . Thus, parallel to works of Refs. 6 and 29, our starting point differs from that of Hooge^{3,30} who argued that the $1/f$ noise due to mobility fluctuations varies inversely with the total number of charge carriers N_e : $\mathbf{s}_m = \text{constant}/N_e$. The conductivity σ_m describes, in general, transport associated with scattering from a disordered and time-dependent part of a system. Constant \mathbf{s}_m depends on temperature (diffusion constant), number of impurities, interaction between them, volume or the area of the component as well as the details related to the scattering process. Our hypothesis is that in a specific sample under fixed external conditions, \mathbf{s}_m remains unchanged, for example even though the sample resistance is changed significantly by enhancing the carrier number by gating. If scattering is anisotropic, then correlations among $1/f$ noise contributions may arise, which yield specific characteristics for the noise when external

conditions are changed (see below). Note that a magnetic field B changes the sample, because the length L of the traversed carrier path becomes longer. Consequently, in the incoherent transport case, the noise due to mobile impurities becomes suppressed as $\mathbf{s}_m \propto 1/L \propto 1/R(B)$.

Conductance in graphene is influenced by immobile impurity scattering, both due to short-ranged and Coulomb scatterers, as well as randomly moving mobile impurities, with the scattering rates proportional to inverse mobilities $1/\mu_s$, $1/\mu_C$, and $1/\mu_m$, respectively. For simplicity, we neglect here the electron-phonon scattering which, however, may govern the inelastic scattering length that is important in electronic interference effects. The graphene conductivity is then given by $\frac{1}{\sigma_g} = \frac{1}{ne} \left(\frac{1}{\mu_C} + \frac{1}{\mu_s} + \frac{1}{\mu_m} \right)$ according to the Mathiessen rule. Consequently, the conductance fluctuation of graphene can be written as

$$S_g(f) = \frac{\langle \Delta \sigma_g^2 \rangle}{\sigma_g^2} = \left(\frac{\sigma_g}{\sigma_m} \right)^2 \frac{\langle \Delta \sigma_m^2 \rangle}{\sigma_m^2} = \left(\frac{\mu_g}{\mu_m} \right)^2 \frac{\langle \Delta \mu_m^2 \rangle}{\mu_m^2} = \left(\frac{\mu_g}{\mu_m} \right)^2 \mathbf{s}_m \frac{1}{f}, \quad (2)$$

where $\frac{1}{\sigma_g} = \frac{1}{ne} \frac{1}{\mu_g}$. The noise of a graphene device thus depends on the electron mobility due to mobile impurity scattering as well as their relative significance in total conductivity given in terms of total graphene mobility μ_g ; if this ratio is modified by some physical process, then the magnitude of the $1/f$ noise changes. For example, if mobile impurities behave as short range scatterers, the mobility related with them may decrease with increasing gate voltage V_g ³¹.

In a typical graphene sample, contact resistance starts to become important at large charge densities at which $\sigma_g \gg G_0$; $G_0 = 2e^2/h$ denotes the conductance quantum. Consequently, $1/f$ noise from contacts has to be taken into account, particularly at large V_g . We model the contact resistance by two parallel transport pathways, one for electrons and one for holes, with conductance G_{ce} and G_{ch} , respectively. We assume that $G_c(n) = G_{ce}(n) + G_{ch}(n) = G_c = \text{const}$. The electrons and holes are treated separately so that their noise is added incoherently, which yields

$$S_c(f) = \frac{\langle \Delta G_c^2 \rangle}{G_c^2} = \frac{\langle \Delta R_c^2 \rangle}{R_c^2} = \frac{n_h^2 + n_e^2}{(n_h + n_e)^2} \frac{\mathbf{s}_c}{f}, \quad (3)$$

where n_e and n_h specify the number density of electrons and holes and we have assigned equally large noise constant \mathbf{s}_c to both carrier species at the two contacts: $S_{ch}(f) = S_{ce}(f) = \frac{\langle \Delta R_{ch}^2 \rangle}{R_{ch}^2} = \frac{\langle \Delta R_{ce}^2 \rangle}{R_{ce}^2} = \frac{\mathbf{s}_c}{f}$. Here $R_c = 1/G_c$ denotes the contact resistance, while its components

$R_{ce} = 1/G_{ce}$ and $R_{ch} = 1/G_{ch}$ specify the contact resistance for electrons and holes, respectively. The density of charge carriers as function of the gate voltage can be estimated as $n = C_g [\sqrt{V_g^2 + V_d^2}]/e$, where the electron-hole crossover voltage scale $V_d \simeq 1.4$ V is close to the residual charge range determined from the measured $G(V_g)$. This V_d scale determines the coexistence of electrons and holes according to $n_{e(h)} = \frac{1}{2}C_g [\sqrt{V_g^2 + V_d^2} + (-)V_g]/e$, which fulfills $n = n_e + n_h$. Note that the constant \mathbf{s}_c has a slightly different role than the constant \mathbf{s}_m since we do not divide the contact resistance into parts according the type of the scattering mechanisms. This is because the contact resistance remains a constant in the range of interest. Near the Dirac point the equation can be approximated as $S_c(f) \approx (1 - 2\frac{n_e n_h}{n^2}) \mathbf{s}_c \frac{1}{f}$ which shows that the noise reaches a minimum at the Dirac point. Without invoking Hooge's law (cf. Refs. 14 and 32), the above equation provides a simple explanation for the noise dip as a consequence of incoherent transport of electrons and holes through a noisy contact resistance.

On the whole, $1/f$ noise in our model is obtained by combing contributions from Eqs. 2 and 3 incoherently. Neglecting the variation of μ_m (though, see below), the noise is described using two fit parameters, \mathbf{s}_m and \mathbf{s}_c , while the rest of the parameters are determined from the conductance $G(V_g)$. Besides these two parameters, we employ a correlation factor χ in order to account for magnetic field dependence of the noise, which clearly indicates the presence of mobility fluctuations: χ describes the correlations between two orthogonal mobility fluctuation components. Using these three parameters we are able to account quite well for our measured noise results covering the parameter range of $|n| < 4 \times 10^{14} \text{ m}^{-2}$ and $0 \leq B < 0.15 \text{ T}$.

II. EXPERIMENTAL SETTING

A scanning electron microscope picture of our graphene Corbino sample with Cr/Au electrodes is illustrated in the inset of Fig. 1: the size of the disk is 4.5 μm in outer diameter and 1.8 μm in inner diameter. The gate voltage dependence of the conductance $G(V_g)$ of our sample at $B = 0$ (see Fig. 1) yielded for the residual charge carrier density $n_0 = 0.5\text{--}1 \times 10^{14} \text{ m}^{-2}$. Details of the sample and its fabrication are discussed in the Methods section.

Our Corbino device displays strong classical, geometric magnetoresistance given by $R_g(B) = R_g(1 + (\mu_0 B)^2) + R_c$ where R_g and μ_0 denote the resistance and mobility of

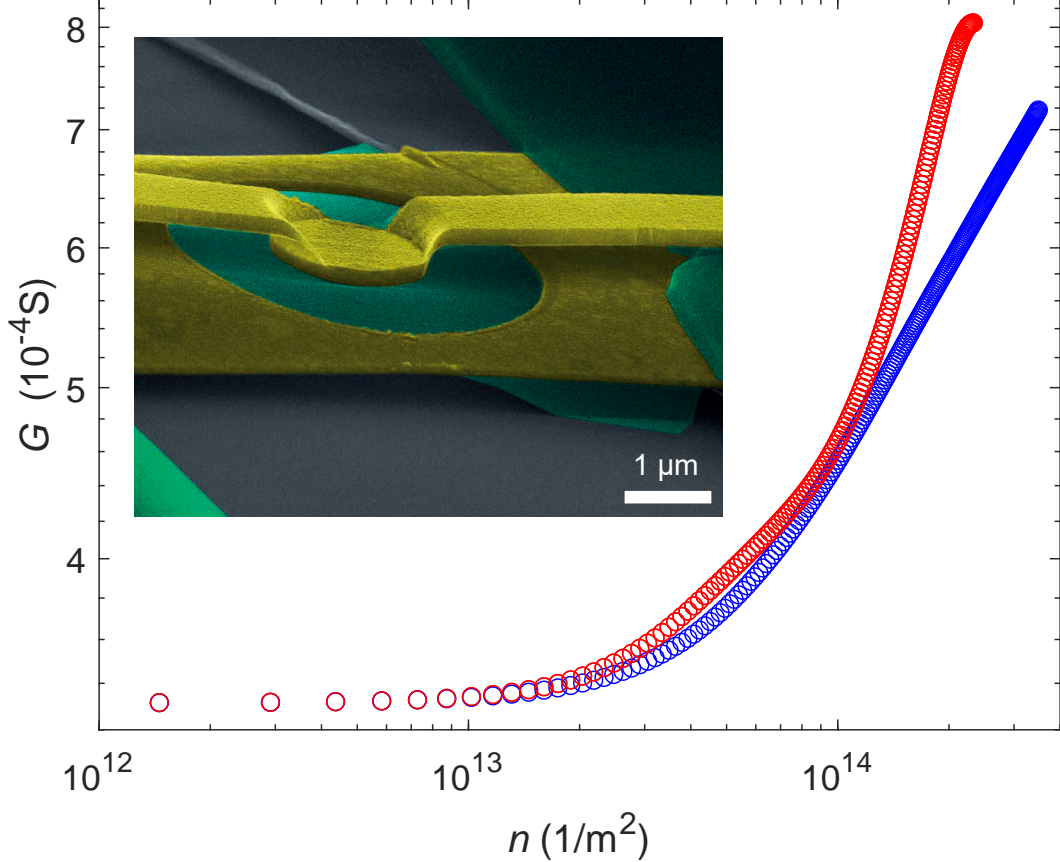


FIG. 1. Zero-bias conductance G vs. charge carrier density n measured at $T = 4.2$ K for $V_g > 0$ (\circ) and $V_g < 0$ (\circ). The inset displays a scanning electron microscope image of our suspended graphene Corbino disk (green part in the center) with $4.5 \mu\text{m}$ diameter outer Cr/Au contact and $1.8 \mu\text{m}$ diameter inner Cr/Au contact. Scale bar for $1 \mu\text{m}$ is given in the image.

graphene at zero field, respectively³¹. Following the analysis of Ref. 31, we determine the contact resistance using the well known diffusive transport modeling for graphene with definite gate dependence for impurity scattering^{31,33} and obtain $R_c \simeq 800 \Omega$, almost independent of gate voltage in the range of gate voltages $V_g = -4 \dots +4$ V. Also, we set $R_{ce} = R_{ch} = R_c$. The slope of the resistance change $\Delta R_g(B)/R_g$ vs B^2 , where $\Delta R_g(B) = R_g(B) - R_g$, indicates that $\mu_0 \simeq 1\text{--}2 \times 10^5 \text{ cm}^2/\text{Vs}$ is approximately constant. The strong B^2 magnetoresistance can also be viewed as a good indicator of the high quality of our sample, as the magnetoresistance in disordered graphene would display more involved field dependence^{34–37}. Since the role of transverse conductivity components vanishes in the Corbino geometry, the mobility is equivalent to that obtained in Hall measurements. Since the ratio of azimuthal ($\hat{\varphi}$) to

radial (\hat{r}) direction currents is given by $i_\varphi/i_r = \mu_0 B$, the current path through the sample is substantially lengthened with growing $\mu_0 B$.

III. RESULTS

Fig. 2a displays measured noise power spectral density S_I vs. frequency f at a few fields between 0 and 0.15 T at $V_g = 10$ V using currents around 5–10 μA . All the data are very close to the pure $1/f$ form: for the data at 0.03 T and $I = 10.2$ μA , for example, fitting of a free exponent β to $1/f^\beta$ yields $\beta = 1.01$. The inset displays a wider frequency scan of the noise at $I = 9.3$ μA : clear $1/f$ noise is present over three decades in frequency. Our data also fulfill the basic properties of $1/f$ noise spectra as a function of bias current $S_I(I) = \mathbf{s} \frac{I^\gamma}{f}$, where $\gamma \sim 2$. The noise magnitude $\mathbf{s} = f \times S_I(I)/I^2 \simeq 2\text{--}5 \times 10^{-10}$ is approximately a constant, which is decomposed into \mathbf{s}_m and \mathbf{s}_c in our analysis. Compared with other low-noise graphene devices, the noise of our sample is on par with the lowest achieved results^{16,38}.

The $1/f$ noise changed irregularly with the increase of magnetic field at low temperatures, in particular at 4 K and below. This is assigned to the role of conductance fluctuations in our sample. Their significance becomes reduced with increasing temperature as the thermal diffusion length $L_T = \sqrt{\frac{\hbar D}{k_B T}}$ decreases from 400 to about 100 nm when T is increased from 4 to 40 K. Consequently, we selected an operation temperature of $T = 27$ K, at which the strength of individual conductance fluctuation features was sufficiently weakened, and the magnetic field dependence could be analyzed better in terms of diffusive transport models.

Charge density dependence of the scaled $1/f$ noise spectral density, $\frac{R_g^2}{R_\Sigma^2} S_I^g/I^2 = \frac{\delta R_g^2}{R_\Sigma^2}$ and $\frac{R_c^2}{R_\Sigma^2} S_I^c/I^2 = \frac{\delta R_c^2}{R_\Sigma^2}$, where $R_\Sigma = R_g + R_c$, is depicted in Fig. 2b for the graphene part and the contacts, respectively. The value for contact noise $S_I^c/I^2 = 3.17 \times 10^{-10}/f$ was determined from data measured at $V_g = -70$ V in the unipolar regime where no pn interfaces exist and $\frac{R_c^2}{R_\Sigma^2} \sim 1$. The data points specified at $f = 10$ Hz were taken from the fits of $1/f$ form to the measured spectra. The open circles denote the experimental data at 27 K, while the filled symbols and the blue curve indicate the separation between the noise contributions from the graphene itself and the contacts, respectively. Clearly, graphene contribution dominates the measured $1/f$ noise at the Dirac point, but at $|n| \sim 4 \times 10^{14} \text{ m}^{-2}$ the graphene contacts account for $\sim 1/3$ of the noise. As the graphene resistance increases with B , the contact contribution in the coupled noise becomes even less significant in a magnetic field. The dip

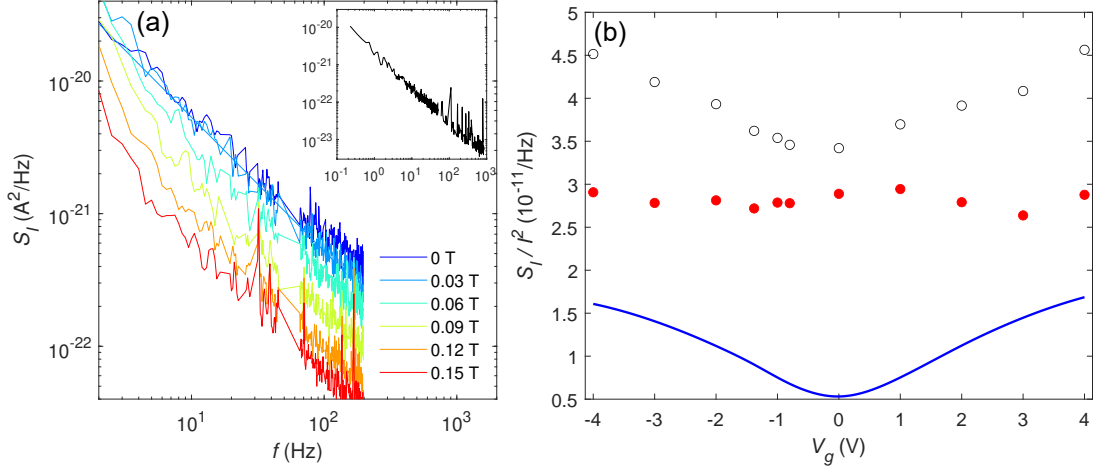


FIG. 2. a) Noise power spectral density S_I vs. frequency f at a few fields between 0 and 0.15 T measured at $V_g = 10$ V and at currents between 3.78 and 10.7 μA ; the current is reduced due to geometric B^2 magnetoresistance. For the data at 0.03 T ($I = 10.2$ μA), the result of $1/f^\beta$ noise fitting with $\beta = 1.01$ is also shown. The inset depicts $1/f$ noise scanned over three decades in frequency at $I = 9.3$ μA . b) Measured (at $T = 27$ K), scaled $1/f$ noise spectral density S_I/I^2 illustrated at 10 Hz as a function of gate voltage V_g (\circ); $|n| < 4 \times 10^{14}$ m^{-2} . The filled circles (\bullet) denote the noise contribution due to graphene resistance fluctuations $\frac{R_g^2}{R_\Sigma^2} S_I^g/I^2 = \frac{\delta R_g^2}{R_\Sigma^2}$ while the solid (blue) curve displays the current noise contribution from contact resistance $\frac{R_c^2}{R_\Sigma^2} S_I^c/I^2 = \frac{\delta R_c^2}{R_\Sigma^2}$.

structure in the noise near the Dirac point is due to the substantial magnitude of S_I^c/I^2 compared with the graphene noise, and it originates from the presence of both electron and hole carriers and incoherent addition of their contact noise contributions.

At small magnetic fields, $B < 0.15$ T, the resistance grows as B^2 and, simultaneously, the apparent Dirac point shifts slightly higher in V_g ³¹. The magnetic field dependence of the measured $1/f$ noise is illustrated in Fig. 3a, which depicts scaled graphene noise power $S_I^g/I^2 = \frac{R_\Sigma^2}{R_g^2} S_I/I^2 - \frac{R_c^2}{R_g^2} S_I^c/I^2$ at 10 Hz as a function of magnetic field B at several charge carrier densities near the Dirac point ($n = -3 \dots +3 \times 10^{14}$ m^{-2}). A clear reduction in noise is observed with increasing B and the reduction takes place in approximately equal relative manner at all gate voltage values. The smallest noise S_I^g/I^2 is observed at the Dirac point, as typical, while the reduction of noise with B becomes strongest at charge densities $n > \pm 1.5 \times 10^{14}$ m^{-2} at which the reduction by the field amounts to $\sim 75\%$. A leveling off of the reduction appears when approaching $B = 0.15$ T, but no clear upturn is found in the investigated

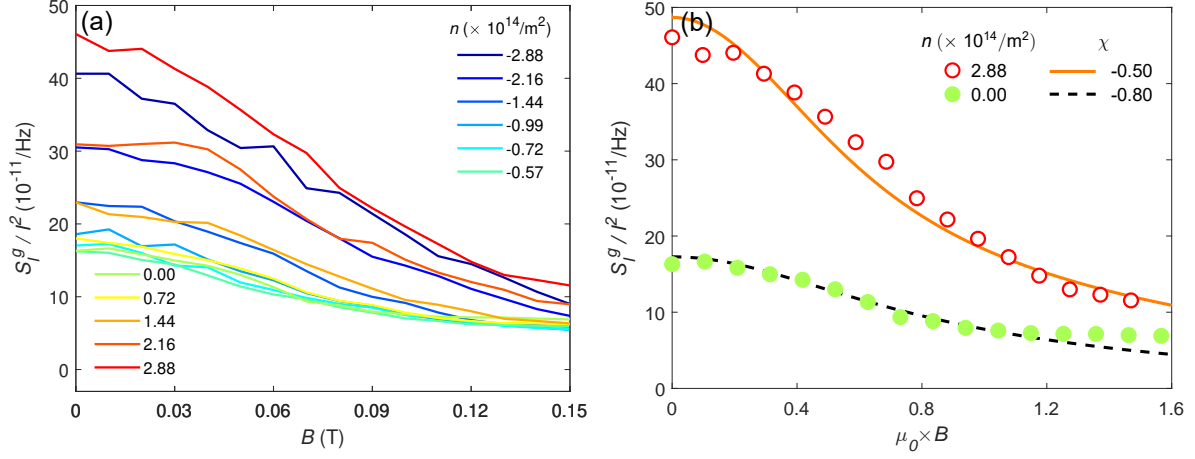


FIG. 3. a) Scaled spectral density of graphene noise S_g^g/I^2 at 10 Hz vs. magnetic field B at various nominal V_g -induced charge densities indicated in the two insets. b) Data at Dirac point (\bullet) and at $n = 2.88 \times 10^{14} \text{ m}^{-2}$ (\circ) plotted as a function of product $\mu_0 \times B$. The dashed and solid curves illustrate theoretical behavior of Eq. (4) using correlation coefficient of $\chi = -0.8$ and $\chi = -0.5$, respectively. Measurement temperature was $T = 27 \text{ K}$.

$B < 0.15 \text{ T}$ range. $B = 0.15 \text{ T}$ was selected as the upper limit in our analysis because there was already a deviation visible from the B^2 dependence in the magnetoresistance $\Delta R/R$.

For Corbino devices with isotropic (scalar) mobility fluctuations $\delta\mu_0$, the current fluctuations should vanish at a sweet spot having $\mu_0 B = 1$. In practice, the sweet spot does not reduce the noise down to zero, but non-idealities/other noise sources will limit the reduction^{23–27}. On the other hand, partial correlations between mobility fluctuations in radial $\delta\mu_r$ and azimuthal $\delta\mu_\varphi$ direction may account for the observed noise reduction. If we simply calculate the total resistance fluctuations as a linear sum of local fluctuations of resistivity we obtain for total resistance fluctuations

$$S_g(f) = \mathbf{s}_m \frac{1}{f} \left(\frac{\mu_g}{\mu_m} \right)^2 \frac{(1 + (\mu_0 B)^4 - 2\chi (\mu_0 B)^2)}{(1 + (\mu_0 B)^2)^2}, \quad (4)$$

where we characterize the combined fluctuations of $\delta\mu_\varphi$ and $\delta\mu_r$ by correlation coefficient χ according to $\langle \delta\mu_\varphi \delta\mu_r \rangle = \chi \langle \delta\mu_r^2 \rangle = \chi \langle \delta\mu_\varphi^2 \rangle$; similar formulas can be derived starting from anisotropic scattering²². When there is full positive (scalar) correlation ($\chi = 1$), the noise vanishes at $\mu_0 B = 1$. With full negative correlation $\chi = -1$, no suppression is seen in the $1/f$ noise^{23–27}. By taking into account $\mathbf{s}_m \propto 1/(1 + (\mu_0 B)^2)$, our results in Fig. 3a yield $\chi \simeq -0.5 \pm 0.1$ away from the Dirac point. This result is in agreement with theoretical

studies for changes in resistance due to reorganization of atoms^{39,40,26} and also with noise correlation measurements in semimetallic Bi⁴¹. According to our own kinetic Monte Carlo simulations (see Methods), the correlation coefficient is $\chi \simeq -0.7$ and -0.4 for $k_B T/E_d = 0.3$ and at $k_B T/E_d = 0.5$, respectively; here E_d is the energy barrier for hopping between sites. The difference in these calculated values for χ can be explained by the fact that, at the lower temperature, a significant number of defects spend a considerable time at the electrodes forming elongated clusters instead of moving freely on graphene without additional restrictions on the shape of clusters as discussed in the supplementary information of Ref. 38.

The gate voltage dependence of $1/f$ noise at $B = 0$ and $B = 0.15$ T is compared in Fig. 4. We observe that the difference between the data at $B = 0$ and $B = 0.15$ T grows monotonically when moving away from the Dirac point. The resistance fluctuations are increasingly suppressed from $B = 0$ value with growing charge carrier density over $|n| = 1 \dots 3 \times 10^{14} \text{ m}^{-2}$. This decrease can be assigned to a small change in the magnitude of correlations between $\delta\mu_r$ and $\delta\mu_\varphi$ from $\chi \sim -0.8$ (at Dirac point) to $\chi \simeq -0.5$ (at $|n| = 3 \times 10^{14} \text{ m}^{-2}$). Possibly, the strengthening in anticorrelation between $\delta\mu_\varphi$ and $\delta\mu_r$ is related to reduced screening at small charge densities.

Graphene properties may also become modified due to external factors, such as strain induced by V_g or local strains induced by adsorption of adatoms⁴². According to Ref. 42, the stress field induced by the adatom extends over till the next nearest lattice sites and it involves asymmetry in the strain distribution. Such strain leads to pseudomagnetic fields⁴³, which act as weak uniform scattering regions. In addition, there arises scalar (gauge) fields which may increase conductivity by enhancing local charge density³⁸. Hence, adsorbed mobile atoms could provide short-ranged scattering centers which cause scalar-type mobility fluctuations, weakening negative correlations. Detailed theoretical modeling of the actual scattering centers and the ensuing $\chi(n)$ is beyond the scope of the present work.

According to Eq. 2, graphene noise at $B = 0$ varies as $\left(\frac{\mu_g}{\mu_m}\right)^2 \mathbf{s}_m \frac{1}{f}$, where the scattering contribution due to mobile impurities, proportional to $1/\mu_m$, may vary with gate voltage. Using diffusive transport theory^{31,33}, scattering by short range impurities produces $1/\mu_s = a|n|$ while for Coulomb impurities $1/\mu_C = b$, where a and b are constants. Using the mobility analysis described in Ref. 31, we can determine μ_g , μ_C and μ_s . The division between relative scattering rates in terms of components μ_C^{-1} and μ_s^{-1} at 27 K is indicated in the

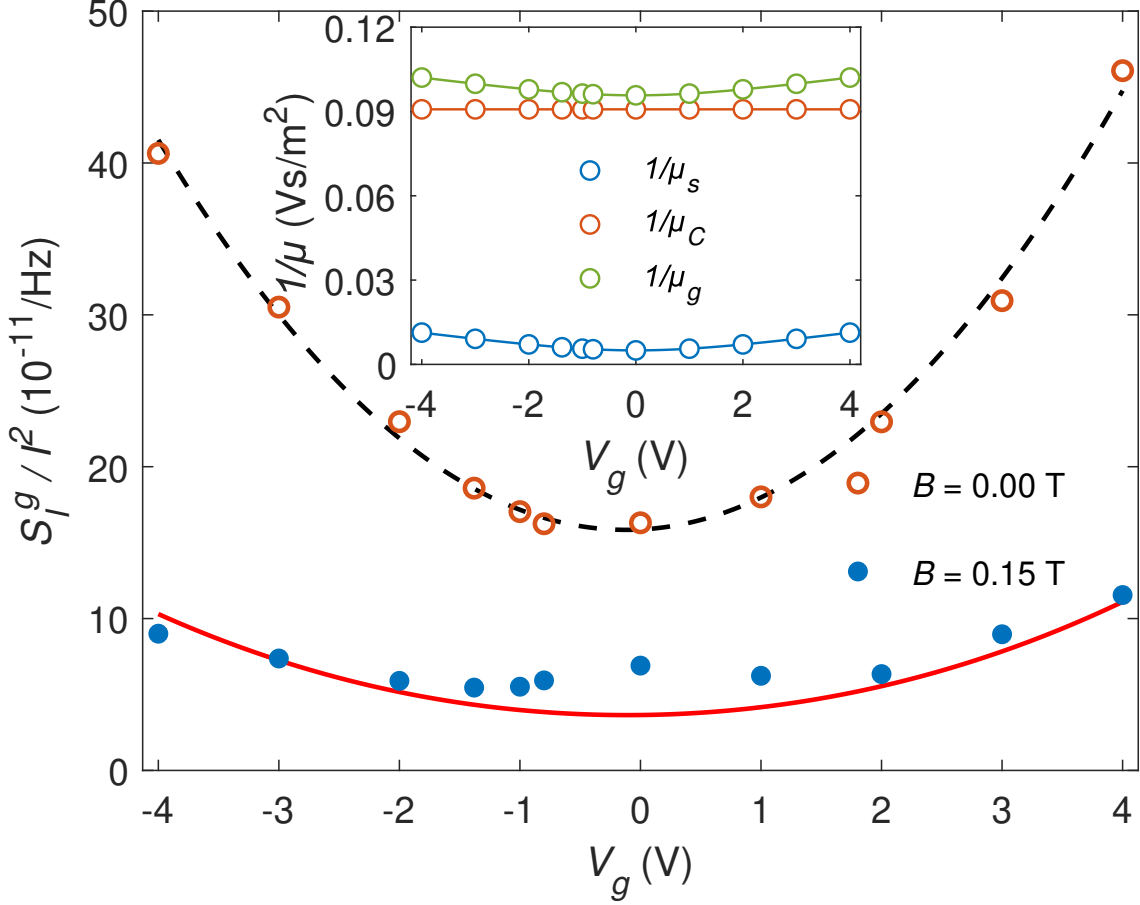


FIG. 4. Scaled graphene noise S_I^g/I^2 at 10 Hz versus gate voltage measured at $B = 0$ (\circ) and at $B = 0.15$ T (\bullet). The dashed parabolic curve on the $B = 0$ data reflects the expected behavior of noise due to the prefactor $\left(\frac{\mu_g}{\mu_m}\right)^2$ in Eq. 2. The solid curve overlaid on $B = 0.15$ T data is calculated using Eqs. 2 and 4 with a fixed $\chi = -0.5$, though slightly stronger anticorrelation is observed near the Dirac point. The inset illustrates V_g dependence of the inverse mobility $1/\mu_g$ determined at 27 K; μ_s and μ_C denote mobility limited by short-ranged and Coulomb scattering, respectively.

inset of Fig. 4. If we assume that mobile impurities would be Coulomb scatterers with constant μ_C , S_I^g would decrease with V_g . Hence we conclude that the majority of mobile impurities in our device must be short range scatterers due to adatoms. For short-ranged scatterers, we obtain a parabolic change of $\left(\frac{\mu_g}{\mu_m}\right)^2$ upto 300...400% across the measured gate voltage range (see Fig. 4). This change will become reduced if part of the scatterers are Coulomb impurities. In fact, the adatoms will produce both short range scattering due to strain and long range scattering due to induced charge at the impurity site. Thus, the

sharp division between short range and long range contributions is not properly valid for the mobile impurities present in our system. Nevertheless, the factor $\left(\frac{\mu_g}{\mu_m}\right)^2$ agrees with the functional form of the measured change, supporting the basic assumption of $\mathbf{s}_m = \text{const.}$ in our $1/f$ noise model. For better testing between theory and experiment, a separate means to determine the scattering contribution of the mobile impurities would be needed.

IV. CONCLUSIONS

We have addressed the fundamental sources of $1/f$ noise in a low-noise, suspended graphene Corbino disk without strong two-level systems. By employing incoherent transport of electrons and holes, we could account for the contact noise by a single parameter. Also, we were able to account for the graphene noise, basically using a single parameter which is related to impurity movement and mobility fluctuations due to random agglomeration/deagglomeration of impurities. The noise decreased with increasing magnetic field, which pinpoints the nature of the noise to mobility fluctuations with intrinsic correlations between radial μ_r and azimuthal μ_φ fluctuations. We find negative orthogonal mobility correlations, which agrees with expectations for "rotating" impurities and our kinetic Monte Carlo simulations. With the significant noise suppression as a function of magnetic field, our work constitutes a strong direct demonstration of mobility noise in two dimensional materials.

Further work is needed to shed light on cluster formation of defects and collective dynamics of such clusters. Recent progress in both metallic and semiconducting 2D materials facilitates good opportunities in tackling these problems. The complex, and possibly self-limiting, dynamics of impurities provides a natural explanation for the long-time memory effects needed to create genuine $1/f$ noise, distinct from the regular $1/f$ noise theories based on distributed two-level or trap states. Our results demonstrate that these collective phenomena may be addressed in very clean micron scale systems.

ACKNOWLEDGEMENTS

We are grateful to Elisabetta Paladino, Igor Gornyi, Manohar Kumar, and Tapio Ala-Nissilä for fruitful discussions and to Sergey Rumyantsev for pointing Ref. [23](#) to us. This

work was supported by the Academy of Finland projects 314448 (BOLOSE), 310086 (LT-noise) and 312295 (CoE, Quantum Technology Finland) as well as by ERC (grant no. 670743). The research leading to these results has received funding from the European Union’s Horizon 2020 Research and Innovation Programme, under Grant Agreement no 824109. The experimental work benefited from the Aalto University OtaNano/LTL infrastructure. A.L. is grateful to Väisälä foundation of the Finnish Academy of Science and Letters for scholarship.

METHODS

All the suspended monolayer graphene devices employed in this work were fabricated using a technique based on lift off resist (LOR) sacrificial layer⁴⁴. Details on our sample fabrication process can be found in Ref. 45. First, graphene was exfoliated on LOR (thickness 500 nm) using a heat-assisted exfoliation technique⁴⁶ and characterized using Raman spectroscopy. Electron-beam lithography was employed to pattern the contacts (5 nm Cr/60 nm Au) using a PMMA 50k/950k double layer resist. A global back gate was provided by the strongly doped silicon Si++ substrate with 285 nm of thermally grown SiO₂ on it. Finally, the samples on LOR were current annealed at low temperatures, typically using a bias voltage of 1.6 ± 0.1 V. Most of the present work was performed on a Corbino disk with an area of $13 \mu\text{m}^2$ and a distance of $1.3 \mu\text{m}$ between the electrodes (inner and outer radii of 0.9 and $2.25 \mu\text{m}$, respectively); a scanning electron microscope picture of a similar Corbino sample is displayed in inset of Fig. 1. The gate capacitance $C_g = 1.5 \times 10^{-5}$ F/m² was obtained using filling factors of Landau levels⁴⁵.

In our experiments, we employed standard voltage-biased measurements for current fluctuations. The current was amplified using a transimpedance amplifier (SR570, gain 10^5) and its fluctuations were measured using a Stanford Research SRS 785 FFT analyzer. For details of our experimental techniques we refer to Refs. 16 and 47.

Kinetic Monte Carlo (kMC) simulations were performed on a model system imitating the Corbino disk geometry by applying appropriate boundary conditions. The calculation procedure and assumptions are described in more detail in Ref. 38. First, the trajectories of the defects on the Corbino disk were generated at two different temperatures ($k_B T = 1.2$ and $k_B T = 2$ while energy barrier for hopping was $E_d = 4$) by the kMC simulations allowing

25 defects to move via thermally activated diffusional hops on a 50 by 50 square lattice. The time evolution of the resistance was then calculated by finite element method (FEM) based on the output of the kMC describing the defect motion on the disk. As suggested by experiments with adsorbed Ne³⁸, the defect sites were assumed to be more conductive than the background lattice. In the present model, the ratio of the conductivity values was set to 10⁵. The FEM calculations were performed for the two orthogonal directions of the current flow, i.e. radial and azimuthal using the same kMC data in both. Finally, a correlation coefficient between the resistance fluctuations in the radial and azimuthal directions was calculated for the two different temperatures.

-
- ¹ S. Kogan, [Electronic Noise and Fluctuations in Solids](#), 1st ed. (Cambridge University Press, New York, NY, USA, 2008).
 - ² T. Grasser, [Noise in Nanoscale Semiconductor Devices](#), edited by T. Grasser (Springer International Publishing, Cham, 2020) pp. 1–729.
 - ³ F. N. Hooge, T. G. M. Kleinpenning, and L. K. J. Vandamme, Experimental studies on $1/f$ noise, [Reports on Progress in Physics](#) **44**, 479 (1981).
 - ⁴ F. N. Hooge, $1/f$ noise sources, [IEEE Transactions on Electron Devices](#) **41**, 1926 (1994).
 - ⁵ S. Feng, P. A. Lee, and A. D. Stone, Sensitivity of the conductance of a disordered metal to the motion of a single atom: Implications for $1/f$ noise, [Physical Review Letters](#) **56**, 1960 (1986).
 - ⁶ J. Pelz and J. Clarke, Quantitative "local-interference" model for $1/f$ noise in metal films, [Physical Review B](#) **36**, 4479 (1987).
 - ⁷ J. Ruseckas, B. Kaulakys, and V. Gontis, Herding model and $1/f$ noise, [EPL](#) **96**, 60007 (2011), [arXiv:1111.1306](#).
 - ⁸ H. J. Jensen, Lattice gas as a model of $1/f$ noise, [Physical Review Letters](#) **64**, 3103 (1990).
 - ⁹ K. S. Ralls and R. A. Buhrman, Defect interactions and noise in metallic nanoconstrictions, [Physical Review Letters](#) **60**, 2434 (1988).
 - ¹⁰ A. A. Balandin, Low-frequency $1/f$ noise in graphene devices., [Nature Nanotechnology](#) **8**, 549 (2013), [arXiv:1307.4797](#).
 - ¹¹ P. Karnatak, T. Paul, S. Islam, and A. Ghosh, $1/f$ noise in van der Waals materials and hybrids, [Advances in Physics: X](#) **2**, 428 (2017).

- ¹² I. Heller, S. Chatoor, J. Männik, M. A. G. Zevenbergen, J. B. Oostinga, A. F. Morpurgo, C. Dekker, and S. G. Lemay, Charge noise in graphene transistors, *Nano Letters* **10**, 1563 (2010).
- ¹³ A. N. Pal, S. Ghatak, V. Kochat, E. S. Sneha, A. Sampathkumar, S. Raghavan, and A. Ghosh, Microscopic mechanism of $1/f$ noise in graphene: Role of energy band dispersion, *ACS Nano* **5**, 2075 (2011).
- ¹⁴ Y. Zhang, E. E. Mendez, and X. Du, Mobility-dependent low-frequency noise in graphene field-effect transistors, *ACS Nano* **5**, 8124 (2011).
- ¹⁵ A. A. Kaverzin, A. S. Mayorov, A. Shytov, and D. W. Horsell, Impurities as a source of $1/f$ noise in graphene, *Physical Review B* **85**, 75435 (2012).
- ¹⁶ M. Kumar, A. Laitinen, D. Cox, and P. J. Hakonen, Ultra low $1/f$ noise in suspended bilayer graphene, *Applied Physics Letters* **106**, 10.1063/1.4923190 (2015).
- ¹⁷ H. N. Arnold, V. K. Sangwan, S. W. Schmucker, C. D. Cress, K. A. Luck, A. L. Friedman, J. T. Robinson, T. J. Marks, and M. C. Hersam, Reducing flicker noise in chemical vapor deposition graphene field-effect transistors, *Applied Physics Letters* **108**, 10.1063/1.4942468 (2016).
- ¹⁸ P. Karnatak, T. P. Sai, S. Goswami, S. Ghatak, S. Kaushal, and A. Ghosh, Current crowding mediated large contact noise in graphene field-effect transistors, *Nature Communications* **7**, 1 (2016).
- ¹⁹ B. Pellegrini, $1/f$ noise in graphene, *The European Physical Journal B* **86**, 373 (2013).
- ²⁰ J. Lu, J. Pan, S. S. Yeh, H. Zhang, Y. Zheng, Q. Chen, Z. Wang, B. Zhang, J. J. Lin, and P. Sheng, Negative correlation between charge carrier density and mobility fluctuations in graphene, *Physical Review B* **90**, 085434 (2014).
- ²¹ P. Dutta and P. M. Horn, Low-frequency fluctuations in solids: $\frac{1}{f}$ noise, *Reviews of Modern Physics* **53**, 497 (1981).
- ²² V. B. Orlov, [Defect Motion as the Origin of the \$1/f\$ Conductance Noise in Solids](#), EUT report 92-E-25 (Eindhoven University of Technology, 1992).
- ²³ M. E. Levinshtein and S. L. Rumyantsev, Noise of the $1/f$ type under conditions of a strong geometric magnetoresistance, *Soviet Physics: Semiconductors* **17**, 1167 (1983).
- ²⁴ M. Song and H. S. Min, Influence of magnetic field on $1/f$ noise in GaAs Corbino disks, *Journal of Applied Physics* **58**, 4221 (1985), <https://doi.org/10.1063/1.335555>.
- ²⁵ M. H. Song, A. N. Birbas, A. van der Ziel, and A. D. van Rheenen, Influence of magnetic field on

- $1/f$ noise in GaAs resistors without surface effects, *Journal of Applied Physics* **64**, 727 (1988), <https://doi.org/10.1063/1.341940>.
- ²⁶ V. Orlov and A. Yakimov, $1/f$ noise in Corbino disk: Anisotropic mobility fluctuations?, *Solid State Electronics* **33**, 21 (1990).
- ²⁷ S. L. Romyantsev, D. Coquillat, R. Ribeiro, M. Goiran, W. Knap, M. S. Shur, A. A. Balandin, and M. E. Levinshtein, The effect of a transverse magnetic field on $1/f$ noise in graphene, *Applied Physics Letters* **103**, 173114 (2013), <https://doi.org/10.1063/1.4826644>.
- ²⁸ D. M. Fleetwood, $1/f$ Noise and Defects in Microelectronic Materials and Devices, *IEEE Transactions on Nuclear Science* **62**, 1462 (2015).
- ²⁹ D. M. Fleetwood and N. Giordano, Direct link between $1/f$ noise and defects in metal films, *Physical Review B* **31**, 1157 (1985).
- ³⁰ F. Hooge, Discussion of recent experiments on $1/f$ noise, *Physica* **60**, 130 (1972).
- ³¹ M. Kamada, V. Gall, J. Sarkar, M. Kumar, A. Laitinen, I. Gornyi, and P. Hakonen, Strong magnetoresistance in a graphene corbino disk at low magnetic fields, *Physical Review B* **104**, 115432 (2021).
- ³² G. Xu, C. M. Torres, Y. Zhang, F. Liu, E. B. Song, M. Wang, Y. Zhou, C. Zeng, and K. L. Wang, Effect of spatial charge inhomogeneity on $1/f$ noise behavior in graphene, *Nano Letters* **10**, 3312 (2010).
- ³³ E. H. Hwang, S. Adam, and S. D. Sarma, Carrier transport in two-dimensional graphene layers, *Physical Review Letters* **98**, 186806 (2007).
- ³⁴ Y. Zheng and T. Ando, Hall conductivity of a two-dimensional graphite system, *Physical Review B* **65**, 245420 (2002).
- ³⁵ M. Müller, L. Fritz, and S. Sachdev, Quantum-critical relativistic magnetotransport in graphene, *Physical Review B* **78**, 115406 (2008).
- ³⁶ J. Jobst, D. Waldmann, I. V. Gornyi, A. D. Mirlin, and H. B. Weber, Electron-electron interaction in the magnetoresistance of graphene, *Physical Review Letters* **108**, 106601 (2012).
- ³⁷ P. S. Alekseev, A. P. Dmitriev, I. V. Gornyi, and V. Y. Kachorovskii, Strong magnetoresistance of disordered graphene, *Physical Review B* **87**, 165432 (2013).
- ³⁸ M. Kamada, A. Laitinen, W. Zeng, M. Will, J. Sarkar, K. Tappura, H. Seppä, and P. Hakonen, Electrical low-frequency $1/f^\gamma$ noise due to surface diffusion of scatterers on an ultra-low-noise graphene platform, *Nano Letters* **21**, 7637 (2021),

<https://doi.org/10.1021/acs.nanoLetters1c02325>.

- ³⁹ J. W. Martin, The electrical resistivity of some lattice defects in FCC metals observed in radiation damage experiments, *Journal of Physics F: Metal Physics* **2**, 842 (1972).
- ⁴⁰ K. E. Nagaev and S. M. Kogan, Low-frequency current noise and internal friction in solids, *Fiz. Tverd. Tela (Leningrad)*, *Sov. Phys. Solid State* **24**, 1921 (1982).
- ⁴¹ R. D. Black, P. J. Restle, and M. B. Weissman, Nearly Traceless $1/f$ Noise in Bismuth, *Physical Review Letters* **51**, 1476 (1983), [arXiv:1011.1669v3](https://arxiv.org/abs/1011.1669v3).
- ⁴² A. V. Krasheninnikov and R. M. Nieminen, Attractive interaction between transition-metal atom impurities and vacancies in graphene: a first-principles study, *Theoretical Chemistry Accounts* **129**, 625 (2011).
- ⁴³ M. I. Katsnelson, *Graphene: Carbon in Two Dimensions* (Cambridge University Press, 2012).
- ⁴⁴ N. Tombros, A. Veligura, J. Junesch, J. J. van den Berg, P. J. Zomer, M. Wojtaszek, I. J. V. Marun, H. T. Jonkman, and B. J. van Wees, Large yield production of high mobility freely suspended graphene electronic devices on a polydimethylglutarimide based organic polymer, *Journal of Applied Physics* **109**, 93702 (2011).
- ⁴⁵ M. Kumar, A. Laitinen, and P. Hakonen, Unconventional fractional quantum Hall states and Wigner crystallization in suspended Corbino graphene, *Nature Communications* **9**, [10.1038/s41467-018-05094-8](https://doi.org/10.1038/s41467-018-05094-8) (2018), [arXiv:1611.02742](https://arxiv.org/abs/1611.02742).
- ⁴⁶ Y. Huang, E. Sutter, N. N. Shi, J. Zheng, T. Yang, D. Englund, H.-J. Gao, and P. Sutter, Reliable exfoliation of large-area high-quality flakes of graphene and other two-dimensional materials, *ACS Nano* **9**, 10612 (2015).
- ⁴⁷ A. Laitinen, M. Kumar, T. Elo, Y. Liu, T. Abhilash, and P. Hakonen, Breakdown of Zero-Energy Quantum Hall State in Graphene in the Light of Current Fluctuations and Shot Noise, *Journal of Low Temperature Physics* [10.1007/s10909-018-1855-x](https://doi.org/10.1007/s10909-018-1855-x) (2018).